셀룰로스 복합소재에서의 수분에 의한 뒤틀림 변형효과를 위한 수치해석적 실험적 연구

김병삼 · 강기준†
호서대학교 기계설계공학과
(2003. 8. 1. 접수 / 2004. 1. 6. 채택)

Numerical Analysis and Experimental Measurement of Hygroscopic Warping Effects for Cellulose Fibres

Byeong-Sam Kim · Kijun Kang†
Department of Mechanical, Hoseo University
(Received August 1, 2003 / Accepted January 6, 2004)

Abstract : The prediction to the hydroscopic moisture warping behaviors is analyzed for cellulose-based laminates using a numerical method base on a modified classical laminate(MCL) theory for hygroscopic moisture deformations with cycling testing data. The experimental measurement of the interferometric hygroscopic warping effects, moisture generator, and curvature of cellulose reinforced epoxy laminates is studied under cyclic environmental conditions using a Moire interferometer coupled. Accurate determination of curvatures provides a description of dimensional stability evolution; the tools for validation of computational internal stress and for the warpage prediction in model safety.

초록 : 본 연구는 셀룰로스 기반의 복합소재에서의 수분 흡수에 의한 뒤틀림 변형효과를 위하여 변형된 고전 선형 적층판 이론을 바탕으로 실험에 의한 반복 데이터 분석 방법과 수치해석의 방법을 이용하여 연구하였다. 실험적 모델은 Moire Interferometer에 따라 수분 생성, 변형과 변형률 모델을 구현하였으며, 실험에 쓰여진 재료는 셀룰로이드 강화 에폭시를 적층한 재료를 사용하였다. 이러한 수치해석에서 제시된 방법으로 내부응력 변화에 따른 변형의 안정성 모델의 평가 툴을 개발하고, 예측모델을 구현할 수 있다.
Key Words : hygroscopic moisture, cellulose-based laminates, numerical method

1. Introduction

Cellulose-based laminated are widely used as mats for resin impregnated laminates essentially because of their ease of impregnation, decorative and surface quality properties and aptness for continuous processes in paper and film industry. Efforts for product development in this long established industry are devoted to improving material durability and surface quality control while increasing production rate. Today, thermoset materials impregnated cellulose mats show excellent surface quality and reasonably fast curing rates, however their dimensional stability as affected by moisture absorption is poor and severely reduces product safety and durability.

The aim of this study is to understand the hygroscopic warping of these systems so as to contribute to the development of dimensionally stable laminates and internal stresses. Because the properties of cellulose fibers as well as their composites are strongly affected by moisture exposure, the behavior of a system at given moisture content does not reflect that of a part in service where the environmental conditions vary regularly. In addition, cellulose fibers show a hysteresis with respect to hygroscopic properties.

These factors make the dimensional stability beha-

† To whom correspondence should be addressed.
kjkang@office.hoseo.ac.kr

vior of cellulose composites quite peculiar and unlike that of inert fiber composites. The main differences lying in the fact that the hygroscopic expansion of cellulose is significant and present both the radial and longitudinal directions, and that the elastic modulus varies significantly between the two extremes of moisture content.

In order to highlight the hygroscopic properties of cellulose mats, extreme cyclic conditioning was performed on the materials investigated, and regularly was followed by Moire interferometer to gather three dimensional deformation maps. The curvatures recorded at different levels of conditioning and of cycling can then be used for describing the service behavior of these materials. In parallel, material property measurements were carried out under the same cyclic environmental conditions in order to gather essential data for numerical simulation. The engineering constants sought were in plane and shear modules and in-plane moisture expansion coefficients, all as a function of moisture content and environmental cycling.

2. Numerical Analysis

2.1. Numerical Formulation

In order to run hydrothermal elastic laminate theory calculations to predict curvatures and internal stresses, a number of engineering constants were evaluated. The analytical models for laminate composite mechanical behavior presented up to now have based on the assumption of constant environmental conditions. Among the many environmental conditions that may influence composite mechanical behavior, changes in temperature and moisture content. The modified lamina stress-strain relationships can be written for linear elastic behavior and constant environmental conditions for an isotropic material.

$$\varepsilon_i^T = \begin{cases} \alpha\Delta T & \text{if } i=1,2,3 \\ 0 & \text{if } i=4,5,6 \end{cases} \tag{1}$$

where α coefficient of thermal expansion (CTE), ε_i^T thermal strains, and ΔT temperature change. Cairns and Adams[1], who have developed cubic polynomial expressions data for epoxy, glass/epoxy, and graphite/epoxy from -73°C to 175°C, base this relationship on the experimental observation.

In polymeric materials moisture has been shown to cause hydroscopic expansions or contractions to thermal strains. The experimental observation is that the moisture-induced strains in isotropic materials can be expressed as

$$\varepsilon_i^M = \begin{cases} \beta\Delta C & \text{if } i=1,2,3 \\ 0 & \text{if } i=4,5,6 \end{cases} \tag{2}$$

where β the coefficient of hygroscopic expansion (CHE), ε_i^M moisture-induced strains, and ΔC moisture concentration.

The total hydrothermal strain can be written as

$$\varepsilon_i^H = \varepsilon_i^T + \varepsilon_i^M \tag{3}$$

The hydrothermal strains in a composite lamina are different in longitudinal and transverse directions. The hydrothermal strains associated with the 12 principal material axes in the specially orthotropic lamina should be expressed as[2]

$$\varepsilon_i^H = \begin{cases} \alpha_i\Delta T+\beta_i\Delta C & \text{if } i=1,2,3 \\ 0 & \text{if } i=4,5,6 \end{cases} \tag{4}$$

If the material is transversely isotropic, $\alpha_2 = \alpha_3$ and $\beta_2 = \beta_3$.

The total hydrothermal strains along the principal material axes in the specially orthotropic lamina are found by summing the hygroscopic strains by Eq. (2) and the thermal strains by Eq. (1).

$$\begin{Bmatrix} \varepsilon_1 \\ \varepsilon_2 \\ \varepsilon_3 \end{Bmatrix} = \begin{Bmatrix} \alpha_1 \\ \alpha_2 \\ 0 \end{Bmatrix} \Delta T + \begin{Bmatrix} \beta_1 \\ \beta_2 \\ 0 \end{Bmatrix} \Delta C \tag{5}$$

Finally, the coefficient of hygroscopic expansion

(CHE) can be expended the matrix formulation with the resultants of hygroscopic forces and moments (if $\Delta T=0$, thermal part is null) as;

$$\begin{Bmatrix} \beta x \\ \beta_y \\ \beta_{xy} \end{Bmatrix} = \begin{bmatrix} a_{xx} & a_{xy} & a_{xs} \\ a_{yx} & a_{yy} & a_{ys} \\ a_{sx} & a_{sy} & a_{ss} \end{bmatrix} \begin{Bmatrix} N_x^H \\ N_y^H \\ N_s^H \end{Bmatrix} + \begin{bmatrix} b_{xy} & b_{xy} & b_{xs} \\ b_{yx} & b_{yy} & b_{ys} \\ b_{sx} & b_{sy} & b_{ss} \end{bmatrix} \begin{Bmatrix} M_x^H \\ M_y^H \\ M_s^H \end{Bmatrix} \quad (6)$$

where, matrix **[a]** and **[b]** are laminate compliance matrices in interlaminar.

The resulting curvature with curvature-moment relationship are given by

$$\begin{Bmatrix} k_x \\ k_y \\ k_{xy} \end{Bmatrix} = \begin{bmatrix} c_{xx} & c_{xy} & c_{xs} \\ c_{yx} & c_{yy} & c_{ys} \\ c_{sx} & c_{sy} & c_{ss} \end{bmatrix} \begin{Bmatrix} N_x^H \\ N_y^H \\ N_s^H \end{Bmatrix} + \begin{bmatrix} d_{xy} & d_{xy} & d_{xs} \\ d_{yx} & d_{yy} & d_{ys} \\ d_{sx} & d_{sy} & d_{ss} \end{bmatrix} \begin{Bmatrix} M_x^H \\ M_y^H \\ M_s^H \end{Bmatrix} \quad (7)$$

where, the matrix **[c]** and **[d]** the laminate stiffnesses by the hydrothermal are meaningful parameters for all laminate configurations.

2.2. Micromechanics Models for Hydrothermal

The mechanical properties of a composite lamina can be estimated from the corresponding properties of the constituent equations for micromechanics models. Similarly, the micromechanics equations for hydrophysical properties appear in hydrothermal have been presented by Chamis[3]. An equation for CTE longitudinal α_1, α_2 can be developed using thermal mechanics model of longitudinal CTEs of fiber and matrix materials. The one-dimensional forms of the stress-strain relationship along the longitudinal direction for the lamina, fiber, and matrix materials were substituted in the rule of mixtures for longitudinal stress[4].

Similarly, the one-dimensional forms of the stress-strain relationship with hydroscopic effects, can be write same procedure above as a found similar relationship for the longitudinal CHE β_1:

$$\beta_1 = \frac{E_{f1}\beta_{f1}v_f + E_{m1}\beta_{m1}v_m}{E_{f1}v_f + E_{m1}v_m} \quad (8)$$

where β_{fl} and β_{ml} are the longitudinal fiber and matrix CHE, E_{fl} and Eml are the Young's longitudinal modulus of fiber and matrix. In polymer matrix composites the amount of moisture absorbed by the fibers is usually negligible in comparison with the moisture absorbed by the matrix, so that the term involving β_{fl} can be ignored. Thus, the transverse CHE β_2 would be given by

$$\beta_2 = (1+v_m)\beta_m v_m + (1+v_f)\beta_f v_f - \beta_1 v_{12} \quad (9)$$

where β_1 is given by the Eq. (8), the equations derived by Schapery.

The example of the hydrothermal micro-properties sensitivity of matrix-dominated is the data of Gibson et *al.*[5], who used a vibration beam method to measure the flexural moduli of several E-glass/polyester sheet-molding compounds after soaking at various times in moisture bath in experimentally.

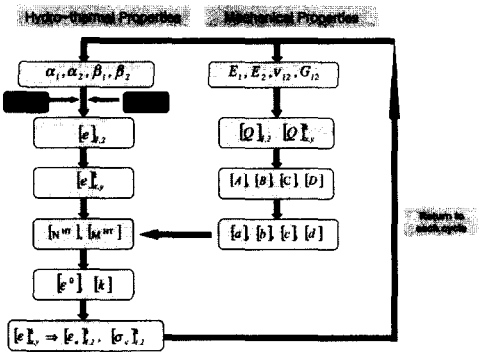

Fig. 1. Flow chart of numerical procedure of hydroscopic model

2.3. Procedure of numerical analysis

In order to run hygro-elastic laminate theory calculations to predict curvatures and internal stresses, a number of engineering constants were evaluated. The procedure consisted in conditioning sample coupons to the same quasi-equlibrium regime as for the Moire measurements, on the flow chart of numerical procedure of hydroscopic model in Fig. 1. The procedure consisted in conditioning sample coupons to the same quasi-equilibrium regime as for the Moire measurements[6]. The material's corresponding moisture content at 90 and 10 % RH at RT, is 9.5 and 3 % (wt./wt.) respectively. Testing was carried out when such moisture contents were reached and was repeated over at least five cycles in order to assess any influence of cyclic conditioning on material properties.

The engineering constants gathered or derived were the machine direction (MD) and cross direction (CD) moduli and the shear MD/CD modulus; the moisture expansion coefficients (CHE) in MD and CD, and the diffusion coefficient Dz. The Fig. 2 and Fig. 3 shows shear modulus values as well as moisture expansion coefficients as a function of environmental cycling. Values calculated according to Baum's relation from E_{MD} and E_{CD}.

MD and CD modules were measured using a Rheumatics solids analyzer RSA II, the out time form the conditioning chamber being minimal and the weight of the coupons being checked before and after testing, moisture loss was kept at a minimum. Shear modulus G_{12} was calculated from E_{MD} and E_{CD} values according to Baum's relation. The coefficients hydroscopic expansion (CHE) was measures using a specially designed fixture with a reading precision of 5mm. The Fig. 4 shows the procedure of moisture measurement until RH generator to Moire interferometer.

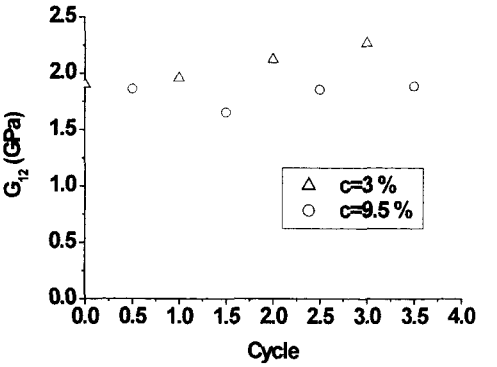

Fig. 2. Evolution of shear modulus during vapour conditioning

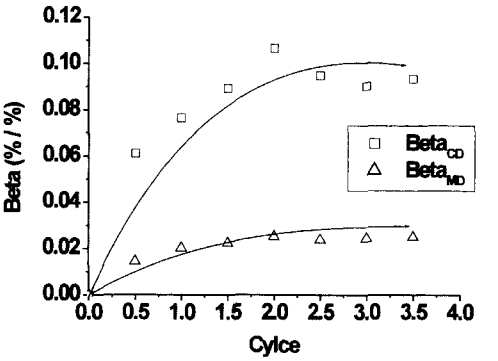

Fig. 3. Evolution of in-plane moisture expansion coefficients (β_{MD} and β_{CD}) during vapour conditioning

3. Experimental

3.1. Moisture Conditioning Procedure

The cured samples were stocked in dry atmosphere subsequent to processing and prior to conditioning. Two types of cycling conditioning were imposed on the specimens; vapor diffusion controlled conditioning, and wet-dry accelerated conditioning. The former was performed with a precise RH generator coupled with a balance to control weight loss and gain for cycles between 10% and 90% RH, providing results on transient and quasi-equilibrium moisture content curva-

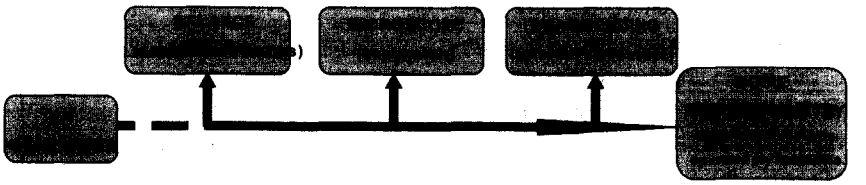

Fig. 4. Procedure of moisture measurement until RH generator to Moire interferometry

tures. For each cycle maximum and minimum moisture content 9.5 and 3% was recorded. The Moire interference method for displacement characterization was chosen as a means to measure deformation[7,8]. This technique relies on the principle that when two closely spaced arrays of parallel lines, which differ in either pitch or orientation, are superimposed and viewed under either transmitted or reflected light, and then interference between the two arrays occurs. In the setup used, an array of lines with a pitch of 20lines/mm was projected at an angle on the warped sample; the reflected, and deformed, array was recorded through a CCD camera fitted with an identical array and placed at the same viewing angle as the projector. This provided a Moire interference pattern, which was further analyzed with Pisa software and transformed into a grey level image; an example of these images is given in Fig. 5 (a) and (b).

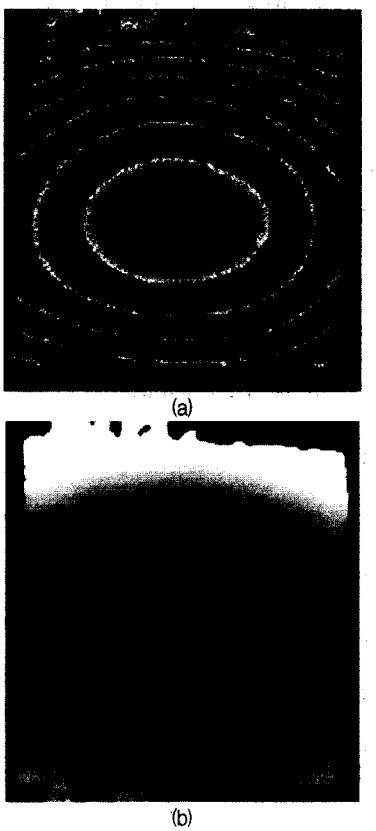

Fig. 5. Examples of Moire pattern images: (a) Moire fringes of a curved surface, (b) Corresponding grey level image.

Depending on the extent of warping of the samples, a less dense array with a pitch of 10lines/mm was used. In fact, when reducing the pitch, the sensibility of the technique is shifted, implying that greater deformations can be measured without saturating the fringes, however sensibility to small strains is reduced. Mounting the sample on a special support performed coupling of the hygroscopic conditioning experiments to Moire interferometer. This latter measure provided neat fringes evenly arising from the centre of the sample irrespectively of the degree of warp.

3.2. Materials

Impregnation of the cellulose mats was carried out manually and each ply was checked for its fiber weight percent at 65%±2%. The cellulose mats were vacuum dried at 80°C overnight before impregnation. Two types of square samples ($80\times80mm^2$) where prepared with 6 pre-pregs; the first stacked in a cross ply lay-up [MD_3; CD_3], and the second stacked in a uniform lay-up [MD_8]. Both laminates were laid up antisymmetrically with respect to the wire and topside of the cellulose mats. Curing was carried out at 165°C for three hours with the samples constrained between Teflon plates both during cure and cool down. The fiber weight percent was only slightly affected by processing due to flow of the resin made in laboratory level. DSC characterization of the pure resin showed full conversion under these curing conditions[9,10].

The cellulose mat used was produced by paper industry. Its main characteristics is a basis weight of $50g/m^2$ ($80\mu m$ thick), an in plane modulus ratio of 3:1 and controlled fiber dispersion. The modulus ratio was chosen to match that of cellulose mats used in industry, where fibres tend to align in the MD of production giving rise to modulus ratios of 2:1 up to 4:1 with respect to the CD. With this in mind, the cellulose mats were treated as orthotropic plies, i.e., also involving an out of plane direction (ZD).

4. Results and Discussion

Fig. 6 show the evolution of the X-axis and Y-axis curvature at the transient moisture content of 6% for

the cross ply laminate as a function of cycling between experimental and numerical . After an initially stable reading, the curvature is seen to rapidly increase and stabilize at approximately twice the warping amplitude. Due to the increase in diffusion coefficient with cyclic exposure as depicted, the transient moisture content of 6% corresponds to an increasingly more uniform moisture content gradient through the thickness. This implies that the hygroscopic deformations about the mid-plane of the laminate are further pronounced hence leading to increased curvature readings. With a stable diffusion coefficient, the curvature amplitude also stabilises. It should be noted that the Y-axis curvature at 6% moisture content is not yet perceivable with the Moire interferometer and appears above 8 % or higher. This is due to the stable curvature configuration being cylindrical and not saddle-shape, i.e., one curvature dominates on the other.

This phenomenon is not accountable by differences in moisture content gradients as the readings are taken at quasi-equilibrium and equilibrium states. Instead an initial or cycle dependant irreversible change of fibre hygrophysical properties is the underlying observable fact. The quantitative observations reported here are bases for validation of numerical predictions, which need to be based on cyclic dependent properties. To this end, work was carried out to assess the nature and magnitude of these changing properties, and hence to implement them in a mechanical model.

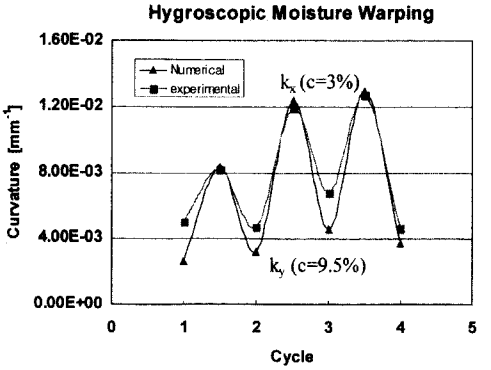

Fig. 6. X and Y curvatures induced by vapour conditioning cycles between 10 and 90 % RH. Line fit representing tendency of curvature evolution

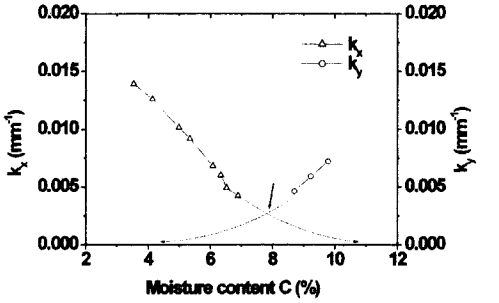

Fig. 7. Evolution of X and Y curvatures induced by vapour conditioning during wetting upon the third cycle

The model used was based on modified classical laminate(MCL) theory accounting for hygroscopic strains. In addition, varying moisture expansion coefficients (CHE) as well as varying modulus values as depicted, were accounted for by implementing a cyclic routine allowing result to be presented in the same manner as those arising from hygroscopic Moire measurements.

The arrow indicates the crossover point where least warping is recorded. During vapor conditioning, curvature values between the two extremes of moisture content were taken at regular intervals for each cycle. The results for a single cycle are summarized in Fig. 7. Each Moire picture taken at the chosen interval provided information on both X-axis and Y-axis curvatures for specific transient moisture content; hence the complete evolution of the part shape was assessed. When at low moisture content, X-axis curvature predominates to the point that Y-axis curvature is invisible to the interferometer.

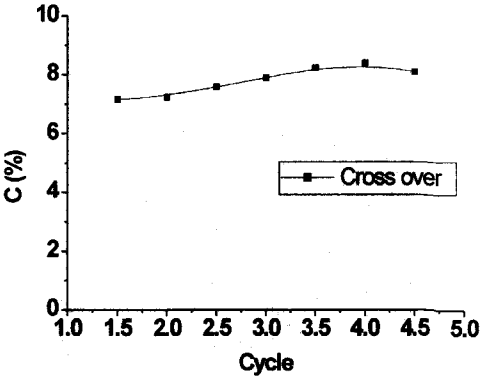

Fig. 8. Progress of crossover point for least warping as a function of cyclic conditioning

The difference in curvature magnitude between the two axes is large enough for the plate to effectively warp into a cylindrical shape, which, upon wetting, gradually flattens. As the moisture content is increased, the X-axis curvature decreases while the Y-axis curvature becomes more evident. At specific moisture content, the two curvatures equate themselves in magnitude.

This crossover point is reflected as a slight warp, and corresponds to the moisture content resulting in the best balance in hygroscopic strains. Following this point, the Y-axis curvature increases while the X-axis curvature falls below the Moire interferometer sensitivity, i.e., the part shows again cylindrical warping, but along the Y axis. The magnitude of cylindrical warp at high moisture contents is lower than at low moisture contents, in fact matrix and fiber soften at high moisture contents increasing the systems compliance and hence deformations are reduced.

It is also interesting to note the evolution of the moisture content for crossover with cycling as depicted in Fig. 8. The change tends towards higher moisture contents in order to obtain a quasi-flat part. This tendency covers an increase of approximately 10% over five cycles. Again confirming that cycling environmental service conditions have a pronounced effect on the dimensional stability of cellulose based composites.

5. Conclusions

The procedure described herein has proven to be a useful tool in observing the deformation behavior of cellulose based composites under environmental cycling. It was found that warping amplitudes evolved with cycling, as did physical properties of the materials in question. In addition environmental conditions for the least possible warping of the cross ply composite were determined and were also found to evolve with cycling. The results presented here are of a phenomenological nature, but nonetheless give insight into the possible mechanisms that govern the dimensional stability of such materials.

References

1) D.S. Cairns and D.F. Adams, "Moisture and thermal expansion properties of unidirectional composite material and the epoxy matrix", Environmental effects on composite materials, Technomic publishing, Lancaster, PA, Vol. 2, pp. 300~316,1984.
2) B. Adl-Zarrabi, "Transient moisture transport in slabs of laminated paper. determination of elastic deformations", 5th Symposium on Building Physics in the Nordic Countries, Finland, 1996.
3) C.C. Chamis, "Simplified composite micromechanics equations for mechnical, thermal, and moisture related properties", Engineer guide to composite materials, ASM international, Vol. 3-8, 1987.
4) I. Chalmers, "The effects of humidity on packaging grade paper elastic modulus," Appita Journal, Vol. 51(1), pp. 25~28, 1998.
5) F. G. Ronald, "Principles of Composite Material Mechanics", McGraw-Hill, Inc., 1994.
6) B-S. Kim et al., "A numerical analysis of the dimensional stability of thermoplastic composites using a thermoviscoelastic composite using a thermoviscoelastic", Journal of Composite material, Vol. 36, No. 20, pp. 2389~2403, 2002.
7) Y. Feng, and O. Suchsland, "Improved technique for measuring moisture contents gradients in wood", Forest Products Journal Technical Note, Vol. 43(3), pp.56-58, 1993.
8) N. Marcovich, et al., "Dependence of the mechanical properties of woodflour-polymer composites on the moisture content", Journal of Applied Polymer Science, Vol. 68, pp. 2069~2076, 1998.
9) W. Simpson, "Determination and use of moisture diffusion coefficient to characterize drying of Northern red oak", Wood Science and Technology, Vol. 27, pp. 409~420, 1993.
10) M. Vanlandinggham et al., "Moisture diffusion in epoxy systems", Journal of Applied Polymer Science, Vol. 71, pp. 787~798, 1999.